

PREFIRE Data User Guide

Auxiliary Satellite Data (AUX-SAT)

Version R01
(20250331)

Kyle Mattingly
Erin Hokanson Wagner
Tim Michaels
Aronne Merrelli

Table of Contents

1	<i>Introduction</i>	3
1.1	Mission Overview	3
1.2	Data Overview	4
1.2.1	Spatial characteristics	4
1.3	Purpose	5
2	<i>Product Description</i>	5
2.1	Algorithm description	6
2.2	File Specifications	8
2.2.1	File naming convention	8
2.2.2	File format	8
2.2.3	Quality flag and bitflags conventions	8
2.2.4	Variables	9
2.2.5	Variable dimensions	9
3	<i>Updates Since Previous Version</i>	13
4	<i>Known Issues</i>	13
5	<i>Resources</i>	15
6	<i>References</i>	15

1 Introduction

This user guide contains information for the PREFIRE data collections PREFIRE_SAT1_AUX-SAT and PREFIRE_SAT2_AUX-SAT, which are archived by the Atmospheric Science Data Center (ASDC) at the NASA Langley Research Center. These collections contain auxiliary satellite data collocated to PREFIRE-TIRS ground footprints for both PREFIRE CubeSats.

1.1 Mission Overview

The Science Mission Directorate (SMD) at NASA Headquarters selected the Polar Radiant Energy in the Far InfraRed Experiment (PREFIRE) as an Earth System Science Pathfinder (ESSP) Earth Venture Instrument (EVI-4) class Mission of Opportunity. Through spectrally resolved observations of radiances spanning the radiatively significant portions of the Mid- and Far-InfraRed (MIR and FIR), PREFIRE addresses two complementary hypotheses:

1. Time-varying errors in both FIR surface emissivity and thermal radiation modulate estimates of energy exchanges between the surface and the atmosphere in the Arctic.
2. These terms are responsible for a large fraction of the spread in projected rates of change for Arctic surface, ocean, and atmosphere characteristics.

These hypotheses are addressed through five related objectives:

- O1.1 Quantify snow and ice FIR emissivity spectra and their variability on seasonal scales;
- O1.2 Quantify the FIR thermal radiation and its response to seasonal variations in cloud cover / water vapor;
- O1.3 Quantify variability in Arctic spectral surface emission and the thermal radiation across the FIR owing to transient cloud and water vapor and sub-daily surface phase-change processes;
- O2.2 Quantify thermal emission errors on projected rates of Arctic warming and sea ice loss;
- O2.3 Determine the impact of improved surface emissivity on modeled ice sheet dynamic processes on hourly scales.

PREFIRE uses broadband infrared ($> 75\%$ of surface emitted thermal radiation) radiance measurements made from the separate orbiting platforms (CubeSats) to address the science objectives. The PREFIRE payloads are two stand-alone instruments built at JPL using heritage from the Mars Climate Sounder and the Moon Mineralogy Mapper. The PREFIRE instruments are thermal infrared imaging spectro-radiometers with more than 50 spectral bands. Each PREFIRE instrument uses ambient temperature thermopile detectors and operates in a pushbroom mode with a point and stare mirror for viewing nadir (Earth), space, and a calibration target. PREFIRE data are calibrated with data from views of the internal calibration target and of space, which are viewed multiple times per orbit.

Soon after launch, the orbit altitude was approximately 531 km for both satellites. However, the PREFIRE CubeSats do not have station-keeping abilities and so their altitudes decrease with time. The current satellite altitude is recorded within the (AUX-SAT) data product files as the *sat_altitude* field (in the *Geometry* data group).

The PREFIRE project delivers space-based measurements of radiative fluxes, cloud masks, spectrally variant surface emissivity (ϵ_λ), and column water vapor (CWV). These are science products with the precision, resolution, and coverage needed to improve our understanding of polar energy balances and Earth-system effects over diurnal and seasonal cycles at scales that capture surface and cloud variability. During its approximately one-year baseline mission, PREFIRE will capture the natural variability in

Arctic and Antarctic CWV and surface temperature. PREFIRE reduces uncertainties in the surface and atmospheric components of the polar energy budget.

1.2 Data Overview

PREFIRE Auxiliary Satellite data are contained in two collections: PREFIRE_SAT1_AUX-SAT and PREFIRE_SAT2_AUX-SAT. The data are provided in distinct data collections because the two PREFIRE-TIRS instruments each have different mission timeframes, observational ground footprints, characteristics, and known issues. Please be sure to read about these differences below.

All Level 1 through Level 3 and Auxiliary PREFIRE data products are produced by the PREFIRE Science Data Processing System (SDPS), located at the University of Wisconsin-Madison. Level 0 data are ingested approximately four times per day for each satellite. Level 1A and 1B Radiance (1A-RAD, 1B-RAD) data products are nominally processed on a delay of at least four days from ingest of the Level 0 science data, allowing for data sent from the spacecraft out of chronological order to be incorporated. The AUX-SAT data products require the observational ground footprint information from the 1B-RAD granules, and are therefore nominally processed just after the 1B-RAD data product granules are produced (the additionally required products from other satellites that are matched to PREFIRE-TIRS ground footprints are typically available with a delay of less than four days from real time).

1.2.1 Spatial characteristics

The PREFIRE-TIRS instruments collect data continuously in a pushbroom mode, with an integration time of 0.7 seconds for each data frame. Each data frame contains a spectral measurement from each cross-track scene collected simultaneously. Within this continuous data collection, there are planned interruptions due to calibration cycles or data downlinks, and there are also occasional interruptions due to unplanned instrument operations changes or outages. Each calibration cycle takes ~18.7 seconds for PREFIRE-TIRS1 and ~9.7 seconds for PREFIRE-TIRS2, which implies a gap of approximately 27 and 14 data frames, respectively. Data downlinks create data gaps of up to 13 minutes, and the exact length varies.

Within the orbital swath there are eight distinct tracks of data associated with the eight separate spatial scenes for each PREFIRE-TIRS. The approximate scene footprint sizes are 11.8 km x 34.8 km (cross-track x along-track), with gaps between each scene of approximately 24.2 km. The swath itself is ~264 km across. Note that the scene footprint and swath sizes quoted here are for the orbit altitude soon after launch. However, the footprint size will slowly become smaller as the orbit altitude decreases with time. Do not assume constant footprint or swath dimensions.

PREFIRE-TIRS spatial footprints overlap each other in the along-track dimension. Assuming that no data are missing, any given point along the orbit swath will be observed by up to about 7 overlapping footprints in the along-track direction. The number of footprints that overlap a given footprint will slowly become smaller during the mission, as the satellites' orbital altitudes decrease. Do not assume an integer number of overlapping footprints.

A single data file or granule consists of data collected during approximately one orbit, beginning and ending near the equator to avoid granule borders over the polar regions. Data files are NetCDF4 format

and approximately 3 MB in size. These data collections are archived at the ASDC DAAC and can be found at https://asdc.larc.nasa.gov/project/PREFIRE/PREFIRE_SAT1_AUX-SAT_R01 and https://asdc.larc.nasa.gov/project/PREFIRE/PREFIRE_SAT2_AUX-SAT_R01.

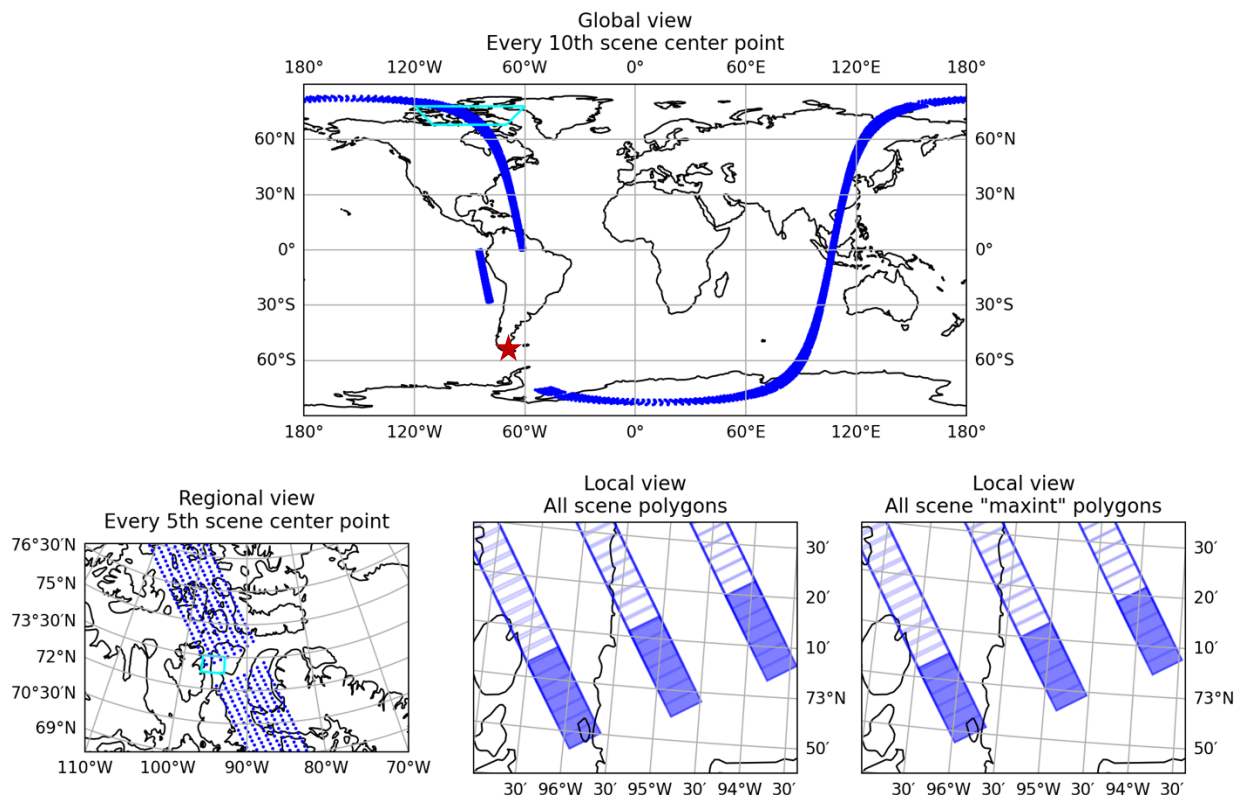


Figure 1-1. An example geolocated orbit (top panel) and focused regional and local plots (bottom panels). The global plot was selected to illustrate a data gap due to a data downlink at the Punta Arenas, Chile ground station, from approximately -70°S to -30°S on the ascending pass at the end of the granule. The zoomed in regional view (lower left) shows the data within the small cyan box in the global plot, and illustrates a smaller data gap due to instrument calibration. The local views (lower middle and right) show the actual scene ground footprint polygons, for the cyan box denoted in the regional view. The first scene's polygon is filled blue, to illustrate the shape of the full field of view (FOV) for one data integration. During the 0.7 second integration time, the satellite moves along track slightly more than 5 km, which means the leading and trailing edges of the instantaneous FOV have translated forward by the same amount. The lower right plot shows the "max integration" footprint polygon, which includes the interior portion of the scene footprint that was within the sensor field of view for the entire integration period.

1.3 Purpose

The PREFIRE AUX-SAT product contains auxiliary satellite products matched in space and time to PREFIRE-TIRS FOVs. These auxiliary data are used to determine the sea ice and snow cover state within PREFIRE-TIRS FOVs and to provide contextual information for scientific analysis of PREFIRE data.

2 Product Description

2.1 Algorithm description

Three auxiliary satellite datasets are matched to PREFIRE-TIRS FOVs using the AUX-SAT algorithm.

(1) The VIIRS Snow Cover Daily L3 Global 0.05Deg CMG, Version 2 product provides the percentage of snow-covered land and cloud-covered land observed daily, within 0.05° (~ 5 km) MODIS/VIIRS Climate Modeling Grid (CMG) cells, from the Suomi-NPP and NOAA-20 JPSS satellites. Due to the fine spatial resolution of this product, many pixels are contained within each PREFIRE-TIRS FOV. Therefore, the statistics in the AUX-SAT VIIRS L3 snow fraction variables are calculated using all “valid” product pixels within each PREFIRE-TIRS FOV that have $< 10\%$ cloud cover, are not experiencing low illumination throughout the day due to polar night, and are not masked by any other product quality flags. Both SNPP and NOAA-20 VIIRS snow cover values are stored in the AUX-SAT output, with the *nviirs* dimension indexing these two satellite platforms for the VIIRS instruments.

(2) The AMSR-E/AMSR2 Unified L3 Daily 12.5 km Brightness Temperatures, Sea Ice Concentration, Motion & Snow Depth Polar Grids, Version 1 product provides sea ice concentration data. Because the spatial resolution of this product is roughly the same scale as the PREFIRE-TIRS FOVs, the sea ice concentration is bilinearly interpolated to PREFIRE-TIRS FOV center points using the ESMPy Python interface to the Earth System Modeling Framework (ESMF) regridding utility after masking land areas and other quality-flagged pixels.

(3) The Near-Real-Time SSM/I-SSMIS EASE-Grid Daily Global Ice Concentration and Snow Extent, Version 5 product (i.e., NISE) provides sea ice concentration and snow cover data with 25 km spatial resolution. As with the AMSR product, the NISE data are bilinearly interpolated to PREFIRE-TIRS FOV center points using ESMPy after masking land (water) areas for the sea ice concentration (snow cover) data. Note that NISE sea ice concentration is provided as a percentage for each pixel while snow cover is a binary value, so the NISE snow fraction value in the AUX-SAT product results from interpolation of binary source values.

As a final step in the AUX-SAT processing, a “final” merged surface type is calculated (*merged_surface_type_final* in the *Aux-Sat* data group). This merged surface type incorporates information from the 1B-RAD *land_fraction* field and several fields from the AUX-MET product (Antarctic land and ice shelf fraction, VIIRS IGBP surface type, and GEOS-IT sea ice and snow cover) along with the auxiliary satellite information processed by the AUX-SAT algorithm.

The method for blending these data sources into a final surface type prioritizes the datasets with the highest spatial resolution first and then prioritizes NOAA-20-sourced over SNPP-sourced snow cover data. For example, to determine snow cover for a PREFIRE-TIRS FOV over land, NOAA-20 snow cover is first checked, and if it is missing, SNPP is checked next, then NISE, and finally GEOS-IT snow cover is used if all other sources are missing. The full logic for determining the final surface type for each PREFIRE-TIRS FOV is shown in the flow chart below (Fig. 2-1). Figure 2-2 illustrates what this field looks like when plotted on a map.

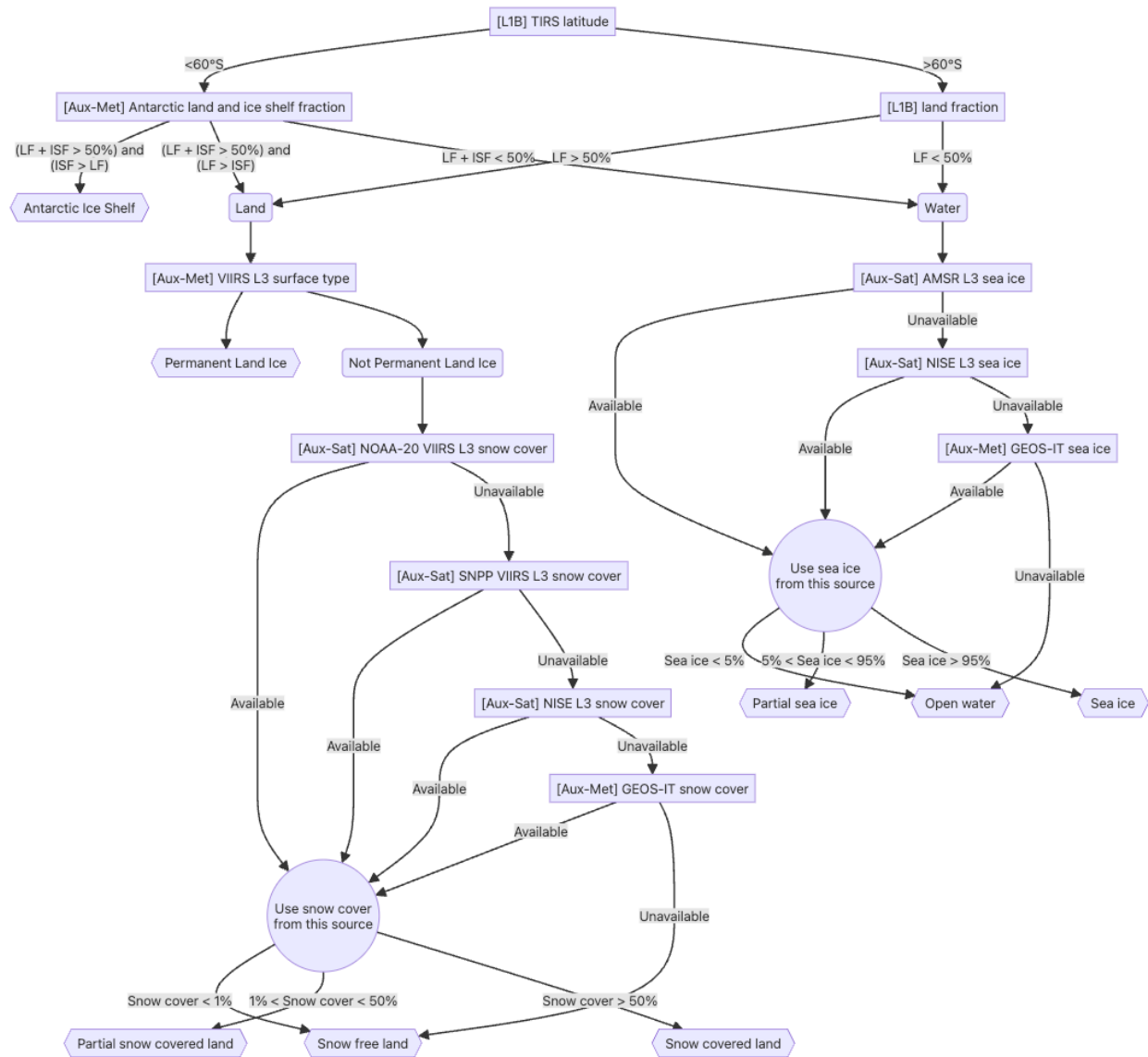


Figure 2-1. Flow chart showing PREFIRE AUX-SAT “final” surface type determination method. Square boxes represent data sources and gray-shaded text represents conditions applied to these data sources. Boxes with rounded edges are intermediate surface type classifications and hexagons are the final output of the algorithm that is stored as the “final” surface type (*merged_surface_type_final*) in the AUX-SAT data product.

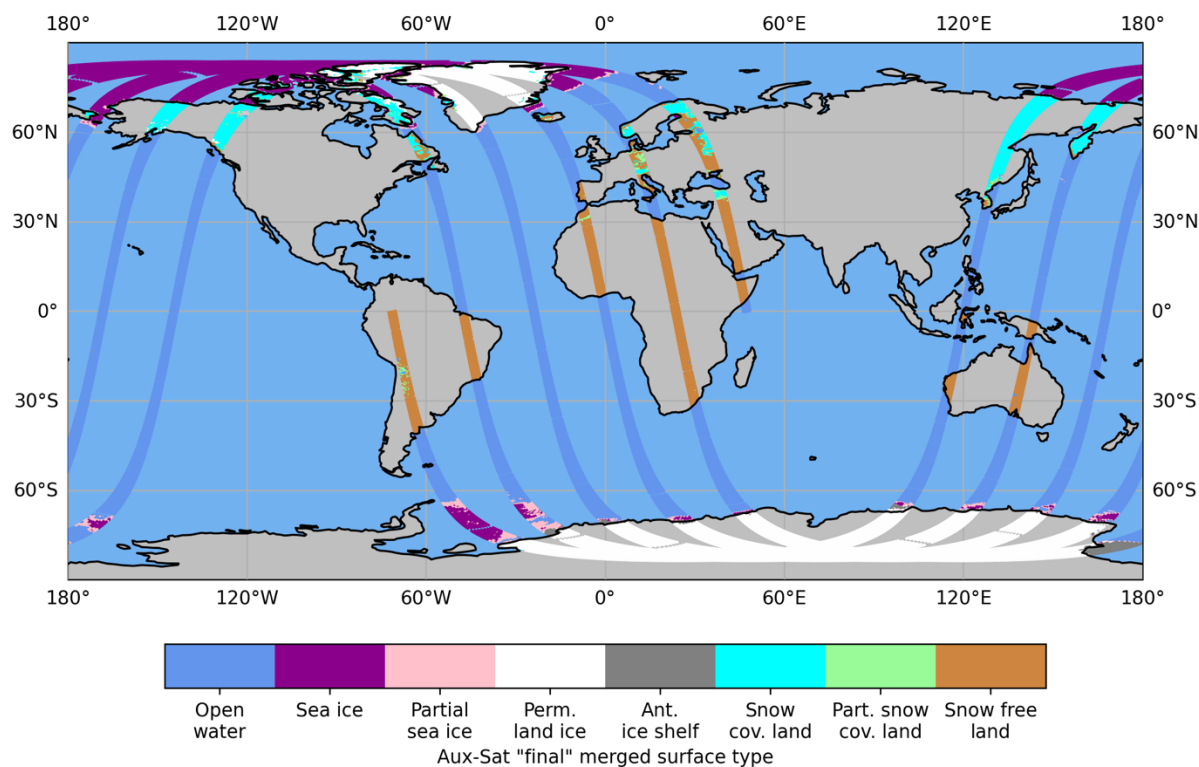


Figure 2-2. “Final” merged surface type from five PREFIRE-SAT2 AUX-SAT granules on 2025-01-07.

2.2 File Specifications

2.2.1 File naming convention

File names for this collection follow the following convention:

PREFIRE_SAT<satID>_<product ID>_<internal product version>_<collection version>_<YYYYMMDDhhmmss>_<granule-ID>.nc

For example, a representative Auxiliary Satellite Data (AUX-SAT) product granule collected by PREFIRE-SAT1 on June 1, 2024 would have the following filename:

PREFIRE_SAT1_AUX-SAT_R01_P00_20240601185321_00123.nc

2.2.2 File format

PREFIRE AUX-SAT data product files are created in NetCDF4 format with standard metadata. These files can be read with standard NetCDF libraries available in all popular scripting languages and many data visualization programs.

2.2.3 Quality flag and bitflags conventions

Because AUX-SAT data are the result of matching external data sources to PREFIRE-

TIRS observation geometry, no unique quality flags are required in the AUX-SAT product. Where PREFIRE-TIRS geolocation data are missing in the upstream 1B-RAD product, AUX-SAT data will also be missing.

2.2.4 Variables

The variable specifications for this collection are described below, with one table devoted to each top-level data group in the NetCDF4 file: *Geometry*, *Aux-Sat*. Note that the *Geometry* group, including all variables, is propagated to every downstream Auxiliary and Level 2 data product from the Level 1B Radiance product (1B-RAD).

2.2.5 Variable dimensions

A summary of all array dimensions is given in Table 2-1. The *xtrack* dimension is equal to the number of cross-track scenes (8, for both instruments), and the *atrack* dimension is equal to the number of along-track Earth observation data frames in the product. The number of along-track frames varies from orbit to orbit, depending on the timing of downlink contacts, calibration data, and other rarer events. Generally, the maximum is around 7700–7900 frames in one product file, with substantially fewer in granules containing downlinks or unplanned instrument/spacecraft events.

Table 2--1

Dimension	Abbreviation
Along-track	<i>atrack</i>
Cross-track	<i>xtrack</i>
VIIRS platform	<i>nviirs</i>
UTC parts	<i>UTC_parts</i> (= 7)
FOV (footprint) vertices	<i>FOV_vertices</i> (= 4)
Dimension label	Definition (C-order)
1D	(<i>atrack</i>)
2D	(<i>atrack</i> , <i>xtrack</i>)
2Du	(<i>atrack</i> , <i>UTC_parts</i>)
3Dj	(<i>atrack</i> , <i>xtrack</i> , <i>nviirs</i>)
3Dv	(<i>atrack</i> , <i>xtrack</i> , <i>FOV_vertices</i>)

2.2.5.1 Geometry group

The *Geometry* data group consists of all timing, observation geometry, and geolocation variables produced during Level-1B processing (see Table 2-2). This data group and its contents will be replicated within any relevant downstream product (e.g., Level-2 data products), rather than stored as a separate geometry file.

Users of NetCDF software packages that try to automatically decode times should be aware that these packages may incorrectly interpret the *ctime* variable as a UTC time. The *ctime* variable is a count of total fractional SI seconds since the epoch 2000-01-01T00:00:00 UTC (i.e., no leap second adjustments since that epoch), while the UTC time standard is adjusted to account for all leap seconds. For example, when the PREFIRE *Geometry* group is read by the `open_dataset` function of the Python `xarray` package using the default `decode_times=True` argument, the resulting *ctime* values (with `datetime64` data type) will differ from the *time_UTC_values* variable by the number of leap seconds that occurred between 2000-01-01T00:00:00 UTC and the observation time. Users of `xarray` and other packages that exhibit this behavior are recommended to use *ctime* along with *ctime_minus_UTC* to calculate UTC times if desired, and/or consult *time_UTC_values* to verify the correct UTC timestamps of PREFIRE observations.

For example, for an `xarray` dataset, a `datetime64` `DataArray` could be computed as follows:

```
import xarray as xr
ds = xr.open_dataset({path_to_1B-RAD_product}, group='Geometry')
ds['UTC_dt64'] = ds['ctime'] - ds['ctime_minus_UTC']
```

Further details on the handling of leap seconds in the CF NetCDF Metadata Conventions can be found in Section 4.4.1 of the CF-1.9 Conventions: <https://cfconventions.org/Data/cf-conventions/cf-conventions-1.9/cf-conventions.html#calendar>.

Table 2--2

Variable Name	Type	Dimension	Units	Description
obs_ID	int64	2D		unique integer identifier for each TIRS look YYYYMMDDhhmmssbtd, composed of UTC date (YYYYMMDD) and time (hhmmss) at TIRS image integration midpoint, t = tenths of seconds [0–9], b = satellite number [1–2], d = scene number [1–8]
ctime	float64	1D	seconds	continuous time since the epoch 2000-01-01T00:00:00 UTC (i.e., similar to TAI) at the midpoint of each TIRS image integration
ctime_minus_UTC	int8	1D	seconds	continuous time minus UTC (i.e., leap seconds since the ctime epoch) at the midpoint of each TIRS image

				integration
time.UTC_values	int16	2Du	various	UTC datetime at the midpoint of each TIRS image integration, represented as an integer array. Array parts: year, month, day, hour, minute, second, millisecond
latitude	float32	2D	degrees_north	topography-corrected latitude of FOV centroid
longitude	float32	2D	degrees_east	topography-corrected longitude of FOV centroid
vertex_latitude	float32	3Dv	degrees_north	topography-corrected latitude for each of the four vertices/corners (arranged counterclockwise starting at the trailing-left corner) of a 4-sided polygon that closely approximates the geolocated FOV (orbital motion taken into account)
vertex_longitude	float32	3Dv	degrees_east	topography-corrected longitude for each of the four vertices/corners (arranged counterclockwise starting at the trailing-left corner) of a 4-sided polygon that closely approximates the geolocated FOV (orbital motion taken into account)
land_fraction	float32	2D		land_area / total_area (remainder is water_area) within the FOV, according to the Digital Elevation Model (DEM)
elevation	float32	2D	m	mean topographic elevation within the FOV
elevation_stdev	float32	2D	m	standard deviation of topographic elevation within the FOV
viewing_zenith_angle	float32	2D	degrees	viewing zenith angle at the FOV centroid
viewing_azimuth_angle	float32	2D	degrees	viewing azimuth angle at the FOV centroid (zero is north, clockwise-positive looking down from the zenith)
solar_zenith_angle	float32	2D	degrees	solar zenith angle at the FOV centroid
solar_azimuth_angle	float32	2D	degrees	solar azimuth angle at the FOV centroid (zero is north, clockwise-positive looking down from the zenith)
solar_distance	float64	2D	km	distance from FOV centroid to the solar barycenter
subsat_latitude	float32	1D	degrees_north	sub-satellite latitude
subsat_longitude	float32	1D	degrees_east	sub-satellite longitude
sat_altitude	float32	1D	km	satellite altitude above the reference ellipsoid (at the sub-satellite point)
sat_solar_illumination_flag	int8	1D		flag specifying whether the spacecraft is illuminated by the sun; 0=no,

				1=partial, 2=full
geoloc_quality_bitflags	uint16	2D		integer composed of bit flags that contain info about the quality of the overall geolocation of each along-track frame of scenes
maxintgz_verts_lat	float32	3Dv		latitude (topography-corrected) for each of the four vertices/corners (arranged counterclockwise starting at the trailing-left corner) of a 4-sided polygon that closely approximates the geolocated zone with the maximum TIRS image integration time
maxintgz_verts_lon	float32	3Dv		longitude (topography-corrected) for each of the four vertices/corners (arranged counterclockwise starting at the trailing-left corner) of a 4-sided polygon that closely approximates the geolocated zone with the maximum TIRS image integration time
orbit_phase_metric	float32	1D	degrees	orbit phase angular metric (range of 0-360 degrees, varying approximately linearly with time), defined as 0 deg at the ascending node (northward equator crossing) of the satellite orbit, 180 deg at the descending node, and so on
satellite_pass_type	int8	1D		flag specifying which type of satellite pass each frame is mostly/all part of. -1 = descending, 1 = ascending

2.2.5.2 Aux-Sat group

Table 2--3

Variable Name	Type	Dimension	Units	Description
VIIRS_L3_num_pts_total	int16	2D		number of VIIRS L3 Climate Modeling Grid (CMG) points within TIRS FOV, including masked points
VIIRS_L3_snow_fraction_num_pts_used	int16	3Dj		number of VIIRS L3 CMG points within TIRS FOV used to calculate snow fraction, after cloud- and quality-flag masking applied
VIIRS_L3_snow_fraction_mean	float 32	3Dj		mean snow fraction across all VIIRS L3 CMG points within TIRS FOV, after cloud- and quality-flag masking applied
VIIRS_L3_snow_fraction_stdev	float 32	3Dj		standard deviation of snow fraction across all VIIRS L3 CMG points within TIRS FOV, after cloud- and quality-flag masking applied

VIIRS_L3_cloud_fraction_num_pts_used	int16	3Dj		number of VIIRS L3 CMG points within TIRS FOV used to calculate cloud fraction, after quality-flag masking applied
VIIRS_L3_cloud_fraction_mean	float32	3Dj		mean cloud fraction across all VIIRS L3 CMG points within TIRS FOV, after quality-flag masking applied
VIIRS_L3_cloud_fraction_stdev	float32	3Dj		standard deviation of cloud fraction across all VIIRS L3 CMG points within TIRS FOV, after quality-flag masking applied
AMSR_L3_seaice_concentration	float32	2D		AMSR L3 sea ice concentration, bilinearly interpolated to TIRS FOV, expressed as a fraction (sea ice area / total water area) ranging from 0 to 1
NISE_L3_snow_fraction	float32	2D		NISE L3 snow cover, bilinearly interpolated to TIRS FOV, expressed as a fraction ranging from 0 to 1. Fraction results from interpolation of binary source data values (0=snow free land, 1=snow covered land)
NISE_L3_seaice_concentration	float32	2D		NISE L3 sea ice concentration, bilinearly interpolated to TIRS FOV, expressed as a fraction (sea ice area / total water area) ranging from 0 to 1
merged_surface_type_final	int8	2D		final merged surface type using met analysis and satellite sea ice and snow cover data 1=open water, 2=sea ice, 3=partial sea ice, 4=permanent land ice, 5=Antarctic ice shelf, 6=snow-covered land, 7=partial-snow-covered land, 8=snow-free land
merged_seaice_final_data_source	int8	2D		sea ice data source used to determine final merged surface type: 0=None, 1=AMSR, 6=NISE, 7=GEOS-IT
merged_snow_final_data_source	int8	2D		snow cover data source used to determine final merged surface type: 0=None, 3=NOAA20 VIIRS L3, 4=SNPP VIIRS L3, 6=NISE, 7=GEOS-IT

3 Updates Since Previous Version

None – this is the initial version.

4 Known Issues

Missing VIIRS snow cover data:

VIIRS L3 daily snow fraction data is missing in areas experiencing low illumination (i.e., polar night) and where clouds obscure the surface. In these common cases, the next product the AUX-SAT algorithm attempts to use to determine snow cover is the NISE L3 product. The snow cover data source used to determine the final surface type for each PREFIRE-TIRS FOV is provided by the *merged_snow_final_data_source* (in the *Aux-Sat* data group) variable.

Geolocation:

The GPS receiver on PREFIRE-SAT1 has performed poorly since launch, and the GPS receiver on PREFIRE-SAT2 ceased to function well at the end of August 2024. Because of the lack of continuously reliable GPS position and time data, the time-dependent orbital position and velocity vectors used for geolocation are based on orbital reconstructions. This uses publicly available orbit element sets (e.g., Two-Line Element sets (TLEs)) based on ranging observations by the United States Space Force and other entities. The precision and accuracy of the orbit reconstruction is currently undergoing evaluation. In addition, residual uncertainties exist due to pointing offsets from lack of precise knowledge of the spectrometer slit orientation relative to the spacecraft. These uncertainties will be addressed after the orbit reconstruction is evaluated and optimized. The current best estimate is that individual geolocated scenes could have along-track geolocation errors of up to 50 km with an average of approximately 30 km (less than the along-track dimension of a ground footprint). The cross-track geolocation error has not been quantified, but the error is likely to be less than the cross-track scene width (approximately 12 km), based on favorable spatial correlations with co-located geostationary imagery collected in the MIR atmospheric window.

As more PREFIRE-TIRS data are collected and analyzed, the quantification of the geolocation biases will improve. Further refinements of the geolocation algorithm are planned, which will reduce these errors in future 1B-RAD data and downstream data product releases.

Electronic pattern noise:

Electrical cross talk between adjacent FPA detectors was largely mitigated by alternating the wiring polarity in the readout integrated circuits. However, residual pattern noise has been noted in both the raw data and the calibrated radiances. This noise is highly temporally correlated and impacts all spectral channels.

This electrical noise manifests in two primary ways. First, “sawtooth-like” patterns can be visible in an individual spectral observation, where the even and odd spectral channels have different radiometric biases. These patterns are generally visible in spectral residuals (observation – modeled radiance). Due to the temporal correlation this pattern could be visible in multiple consecutive frames. Second, “striping” is visible when data from a selected channel are viewed spatially, where specific spatial scenes are clearly biased relative to the other scenes. Again, due to the temporal correlation these stripes will continue along track for some time. No data flagging is performed related to this pattern noise effect, but future developments in the calibration algorithm are planned to further reduce this noise.

5 Resources

For more information, contact Erin Hokanson Wagner at prefire-sdps.admin@office365.wisc.edu.

6 References

Brodzik, M. J. and J. S. Stewart. (2016). Near-Real-Time SSM/I-SSMIS EASE-Grid Daily Global Ice Concentration and Snow Extent, Version 5 [Data Set]. Boulder, Colorado USA. NASA National Snow and Ice Data Center Distributed Active Archive Center. <https://doi.org/10.5067/3KB2JPLFPK3R>. Date Accessed 03-27-2025.

L’Ecuyer, T.S., Drouin, B.J., Anheuser, J., Grames M., Henderson, D., Huang, X., Kahn, B.H., Kay, J.E., Lim, B.H., Mateling, M., Merrelli, A., Miller, N.B., Padmanabhan, S., Peterson, C., Schlegel, N.-J., White, M.L., Xie, Y., “The Polar Radiant Energy in the Far-InfraRed Experiment: A New Perspective on Polar Longwave Energy Exchanges,” *Bulletin of the American Meteorological Society (BAMS)*, 102(7), E1431–E1449, 2021.

Meier, W. N., T. Markus, and J. C. Comiso. (2018). AMSR-E/AMSR2 Unified L3 Daily 12.5 km Brightness Temperatures, Sea Ice Concentration, Motion & Snow Depth Polar Grids, Version 1 [Data Set]. Boulder, Colorado USA. NASA National Snow and Ice Data Center Distributed Active Archive Center. <https://doi.org/10.5067/RA1MIJOYPK3P>. Date Accessed 03-27-2025.

Padmanabhan, S., Drouin, B., L’Ecuyer T., White, M., Lim. B., Kenyon, M., Mariani, G., McGuire J., Raouf, N., De Santos, O., Bendig, R., “The Polar Radiant Energy in the Far-InfraRed Experiment (PREFIRE),” *IGARSS 2019 – 2019 IEEE International Geoscience and Remote Sensing Symposium*

Riggs, G. and D. K. Hall. (2023). VIIRS/NPP Snow Cover Daily L3 Global 0.05Deg CMG, Version 2 [Data Set]. Boulder, Colorado USA. NASA National Snow and Ice Data Center Distributed Active Archive Center. <https://doi.org/10.5067/PHOQ2G589HCC>. Date Accessed 03-27-2025.

Riggs, G. and D. K. Hall. (2023). VIIRS/JPSS1 Snow Cover Daily L3 Global 0.05Deg CMG, Version 2 [Data Set]. Boulder, Colorado USA. NASA National Snow and Ice Data Center Distributed Active Archive Center. <https://doi.org/10.5067/DNC2SNXE6HJB>. Date Accessed 03-27-2025.

Citation

DOI:

- PREFIRE_SAT2_AUX-SAT_R01: 10.5067/PREFIRE-SAT2/PREFIRE/AUX-SAT_L3.R01
- PREFIRE_SAT1_AUX-SAT_R01: 10.5067/PREFIRE-SAT1/PREFIRE/AUX-SAT_L0.R01